The Limits of Promiscuity: Isoform-Specific Dimerization of Filamins†

Mirko Himmel,‡ Peter F. M. van der Ven,‡ Walter Stöcklein,§ and Dieter O. Fürst*,‡

Department of Cell Biology, University of Potsdam, Lennéstrasse 7a, 14471 Potsdam, Germany, and Department of Analytical Biochemistry, University of Potsdam, P.O. Box 601553, 14415 Potsdam, Germany

Received July 24, 2002; Revised Manuscript Received October 30, 2002

ABSTRACT: Filamins are a family of actin cross-linking proteins that are primarily localized in the cortical cytoplasm of all mammalian cells. Until now, three major isoforms (filamins a, b, and c) have been identified, that were shown to be differentially expressed and/or localized in different tissues. An amino-terminal double CH-domain actin binding domain, and a dimerization region in the carboxy-terminal portion of the protein are the molecular basis for its actin cross-linking activity. Chemical cross-linking of bacterially expressed recombinant proteins was used to demonstrate that in all three filamin isoforms the most carboxy-terminally situated immunoglobulinlike domain is required and sufficient for dimerization. The efficiency of the dimerization was increased upon inclusion of the preceding hinge 2 region, indicating a function for this region in the regulation of dimerization. By mixing recombinant proteins derived from different filamin isoforms, we found that heterodimer formation is possible between filamins b and c but not between filamin a and the other two filamins. This selectivity of dimerization might provide a further molecular explanation for the differential intracellular sorting of filamin isoforms and their distinct properties.

A multitude of cellular processes involves complex and dynamic reorganization of the actin cytoskeleton. All of these events are guided by the activity of a large number of actin binding proteins. While the monomer−polymer transition of actin is influenced by monomer sequestering, filament-severing and filament-capping proteins, the shape and thus the detailed functionality of the structures formed by F-actin is determined by filament cross-linking proteins. An important subgroup of the latter that seems particularly involved in reshaping the actin cytoskeleton and its associated structures is the filamins. Actin binding in the filamins is conferred by an amino-terminal region consisting of two CH domains (*1*), while the remainder of the ~280 kDa polypeptide specifies both dimer formation and binding to a plethora of filamin-binding proteins. These include on one hand integrin receptors, channels, and other transmembrane proteins and on the other hand several signaling proteins. Thus, the cellular activities of filamins include the organization of membrane protein complexes and a scaffolding role for several signaling pathways in numerous different cell types (for reviews see, e. g., refs 2 and 3). Their general importance is impressively demonstrated by the fact that mutations in human filamin genes cause the neuronal migration disorder periventricular heterotopia (*4*) and possibly also the skeletal muscle disease LGMD1E, a subtype of limb girdle muscular dystrophy (*5*).

The molecular basis for this striking functional complexity is—at least in part—the existence of three paralogous filamin genes in the human genome, each giving rise to differentially spliced variants (see ref 6 and references therein). Only recently a new nomenclature for the filamin family was introduced, giving account to the order in which complete sequence data entered the human genome database (*2*). Accordingly, the first filamin isoform, originally described as actin binding protein (*7*) or filamin (*8*), that was fully sequenced (*9*) is now called filamin a. The second filamin sequenced to completeness was renamed from β-filamin or ABP-278 (*10*, *11*, *12*) to filamin b. The variant predominating in striated muscle tissue, originally described as ABP-like protein (*13*) and subsequently as γ-filamin (*14*) was thus designated filamin c.

The Y-shaped structure of purified filamin observed in the electron microscope following rotary shadowing (*9*, *15*) or negative staining (*16*) presented evidence for the ability of filamins to dimerize. Biochemical studies, which were performed solely with filamin a, hinted at an involvement of the carboxy-terminal immunoglobulin-like (Ig-like) domain in filamin dimer formation; however, the evidence was of a rather indirect nature (*9*, *17*). The more recent unequivocal identification of several filamin variants (see above), and the concomitant observation that different filamin isoforms are coexpressed in a single cell type, urged us to investigate precisely which molecular portion is necessary and sufficient for dimer formation of all filamins and whether different filamin variants are able to form heterodimers. Thus, our analysis revealed that bacterially expressed and purified carboxy-terminal Ig-like domain 24 of all filamins was necessary and sufficient for dimerization in vitro. However, the inclusion of the preceding insertion (hinge 2 region) significantly enhanced the ability of the domains to dimerize. In addition, we found that filamins b and c may also form heterodimers, at least in vitro, while filamin a was only

† This study was supported by a grant from the Deutsche Forschungsgemeinschaft to D.O.F.

* To whom correspondence should be addressed: phone +49 331 977 48 73; fax +49 331 977 48 61; e-mail dfuerst@rz.uni-potsdam.de.

‡ Department of Cell Biology, University of Potsdam.

§ Department of Analytical Biochemistry, University of Potsdam.

10.1021/bi026501+ CCC: $25.00
Published on Web 12/21/2002

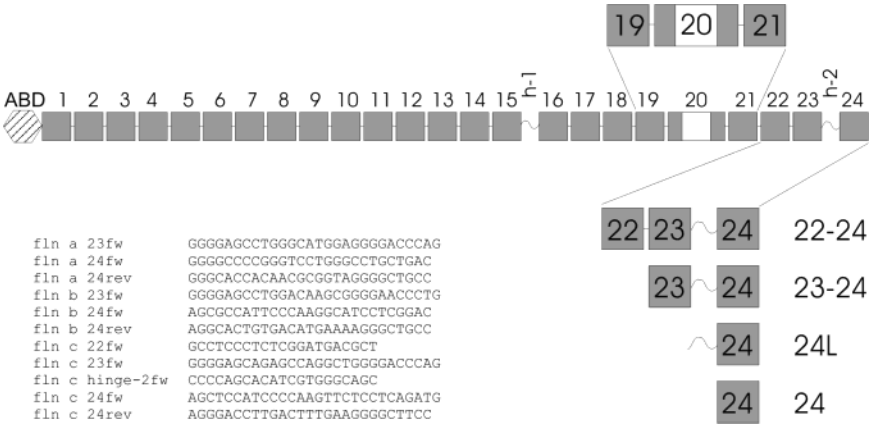

FIGURE 1: Schematic representation of the domain structure of the filamins. In all filamin isoforms an amino-terminal actin-binding domain (ABD) is followed by 24 Ig-like domains. Interdomain insertions are found between Ig-like domains 15 and 16 (hinge 1) and 23 and 24 (hinge 2). The hinge 1 region is alternatively spliced in at least filamins b and c. Further alternative splice variants were described, but none of them were in the carboxy-terminal regions. The muscle-specific isoform filamin c carries a unique insertion in its Ig-like domain 20. The recombinant polypeptides that were used for the dimerization experiments described in this report and the sequence of the primers used for cloning the truncated cDNAs in the pET vectors are indicated.

capable of forming homodimers. This report therefore provides a molecular basis for further studies at the cellular level.

MATERIALS AND METHODS

Construction of Expression Constructs. Total RNA was extracted from nondifferentiated and differentiated human skeletal muscle cells grown in culture (*18*) by a single-step extraction method (RNA NOW; Biogentex, Seabrook, TX). Specific fragments of the nonmuscle filamin isoform (filamin a) or the muscle-specific filamin isoform (filamin c) cDNAs were obtained by RT-PCR[1] with Expand reverse transcriptase for first-strand synthesis and the Expand long-template PCR system, both according to the instructions of the manufacturer (Roche Molecular Biochemicals, Mannheim, Germany). For amplification of filamin b cDNA fragments, the complete filamin b cDNA (kindly provided by Drs. Shapiro and Takafuta, Cardeza Foundation for Hematologic Research, Philadelphia, PA) was used as a template. The positions of the amplified fragments and the sequences of the primers used for amplification of the cDNA fragments are given in Figure 1. Truncated cDNA fragments were cloned either into the prokaryotic expression vector pET23-EEF, resulting in fusion proteins carrying a carboxy-terminal His_6 tag and an EEF immunotag (*19*; see below), or into pET23-T7 (amino-terminal T7 tag and carboxy-terminal His_6 tag (*20*). The integrity of the constructs was verified by DNA sequencing (Sequence Laboratories, Göttingen, Germany, or Agowa, Berlin, Germany).

Antibodies. Since recombinant proteins were either tagged amino-terminally with a peptide of the bacteriophage T7 major capsid protein (T7 tag) or carboxy-terminally with the amino acids EEF, fusion proteins could be detected either by a monoclonal antibody (mAb) specific for the T7 tag (Novagen, Heidelberg, Germany) or by the rat mAb YL1/2 (*21*; a kind gift of Dr. J. Wehland, Braunschweig, Germany), respectively.

Protein Expression and Purification. Protein expression in *Escherichia coli* BL21(DE3)pLysS (Novagen, Heidelberg, Germany) was performed as described (*19*, *20*, *22*). His-tagged proteins were purified by use of the QiaExpress kit as described by the manufacturer (Qiagen, Hilden, Germany). Briefly, bacterial cells were precipitated and lysed by addition of lysis buffer (50 mM sodium phosphate, pH 8.0, 300 mM NaCl, 10 mM imidazole, and 1 mg/mL lysozyme). DNA was fragmented by sonification and cell debris was sedimented by centrifugation (18000*g*, 30 min, 4 °C). The supernatant containing the soluble fraction of recombinant polypeptide was incubated with Ni^{2+}−NTA agarose beads with constant agitation for 1 h at 4 °C. After the agarose beads were placed into a column, they were washed twice with washing buffer (50 mM sodium phosphate, pH 8.0, 300 mM NaCl, and 20 mM imidazole) and bound protein was eluted with elution buffer (50 mM sodium phosphate, pH 8.0, 300 mM NaCl, and 250 mM imidazole). Protein solutions were dialyzed overnight against CL buffer (80 mM NaCl, 20 mM NaP_i, pH 7.0, 1 mM $MgCl_2$, and 1 mM DTT) and subsequently stored on ice. Protein concentrations were determined with the Bio-Rad protein assay dye reagent.

CD Spectroscopy. To show the integrity of the expressed proteins, their secondary structure was analyzed by CD spectroscopy. Recombinant fragment fln c 23−24 was dialyzed against 50 mM sodium phosphate buffer (pH 7.0) and diluted to 1 mg/mL. The extinction coefficient of the filamin fragment was determined as described (*23*) and the molar protein concentration was calculated according to the law of Lambert−Beer. CD spectra were recorded in the far UV in thermostated cells (20 °C) with light paths of 0.1 and 1 mm, on a Jasco J-715 spectropolarimeter. Ten scans were averaged. The mean molar residue ellipticity was plotted against the wavelength.

Chemical Cross-Linking Assays. Recombinant protein fragments of different filamin isoforms (Figure 1) were diluted to a final concentration of 4 μM in CL buffer containing 0.6 M KCl. After 1 h of incubation on ice, the cross-linker ethylene glycol bis(succinimido succinate) (EGS, dissolved in DMSO) was added to a final concentration of

[1] Abbreviations: DTT, dithiothreitol; EGS, ethylene glycol bis(succinimido succinate); Ig-like, immunoglobulinlike; mAb, monoclonal antibody; PBST, phosphate-buffered saline with Tween-20; PVDF, poly(vinylidene difluoride); RT-PCR, reverse transcriptional polymerase chain reaction; RU, relative units; SDS−PAGE, sodium dodecyl sulfate−polyacrylamide gel electrophoresis; SPR, surface plasmon resonance; TCA, trichloroacetic acid.

Table 1: Nomenclature and Size of the Recombinant Filamin Fragments

name	filamin isoform	tags	Ig-like domains	calculated molecular mass (kDa)	apparent molecular mass (kDa)
fln a 23−24	a	His_6, T7	23 and 24	26.3	30
fln a 24	a	His_6, EEF	24	12.2	16
fln b 23−24	b	His_6, T7	23 and 24	26.7	30
fln b 24	b	His_6, EEF	24	11.9	16
fln c 22−24	c	His_6, EEF	22 to 24	39.3	40
fln c 23−24	c	His_6, T7	23 and 24	26.5	30
fln c 24L	c	His_6, EEF	hinge 2 + 24	19.3	22
fln c 24	c	His_6, EEF	24	12.5	16

1.3 mM and samples were incubated at 37 °C for 20 min. The cross-linking reaction was stopped by precipitating the protein with 10% TCA (final concentration), and after 30 min of incubation on ice the protein was collected by centrifugation (18000*g*, 4 °C, 15 min). Pellets were washed once with 80% acetone and once with pure acetone. Acetone was removed by air-drying at room temperature. Proteins were dissolved in hot SDS sample buffer, boiled for 2 min, and analyzed by SDS−PAGE (*24*).

Western Blotting. Polyacrylamide gels were blotted onto PVDF membranes by use of a semidry transfer cell (Bio-Rad Laboratories, Munich, Germany) and a discontinuous buffer system [anodic buffer I, 300 mM Tris base and 20% (v/v) methanol, pH 10.4; anodic buffer II, 25 mM Tris base and 20% (v/v) methanol, pH 10.4; cathodic buffer, 40 mM 6-aminocapronic acid and 20% (v/v) methanol, pH 7.6]. Membranes were stained with Coomassie-based Gel Code (Pierce, Rockford, IL).

Immunodetection. PVDF membranes were blocked and incubated by standard procedures. The peroxidase-conjugated secondary antibodies were purchased from Jackson Immuno Research Laboratories (West Grove, PA) or American Qualex (San Clemente, CA). Conjugated enzymes were detected by enhanced chemiluminescence with SuperSignal West Pico chemiluminescent substrate (Pierce, Rockford, IL) and Kodak XAR-351 film. For multiple immunodetections, primary and secondary antibody complexes were removed from the PVDF membranes in stripping buffer [200 mM glycine hydrochloride, pH 2.2, 20 mM DTT, 0.1% (w/v) SDS, and 1% (v/v) Tween-20] at room temperature. Membranes were washed thoroughly with PBST before each subsequent immunodetection.

Surface Plasmon Resonance. Surface plasmon resonance (SPR) analysis, in a Biacore 2000 instrument equipped with a nitrilotriacetic acid (NTA) sensor chip, control software version 2.1, and evaluation software version 3.0 (Biacore AB, Uppsala, Sweden), was applied to confirm that filamin fragments dimerize in the absence of a cross-linking reagent. His_6-tagged recombinant filamin fragments were bound to saturation on the sensor chip via chelated nickel under experimental conditions that either allow filamin dimerization (20 mM sodium phosphate, pH 7.0, containing 80 mM NaCl and 10 μM EDTA) or prevent dimerization (20 mM sodium phosphate, pH 7.0, containing 80 mM NaCl, 600 mM KCl, and 10 μM EDTA; see below). To minimize rebinding of dissociated filamin to the chip in the early phase of dissociation, the histidine binding sites of the nickel-chelated chips were saturated with the recombinant polypeptide. Subsequently, the chips with bound filamin fragments were washed in buffer with or without KCl. A reduction of the resulting SPR signal during washing would indicate a dissociation of filamin dimers, and thus the presence of filamin dimers on the chips. Each assay cycle consisted of the following steps: (a) injection of 50 μL of $NiSO_4$ (1 mM in H_2O); (b) injection of 10 μL of filamin fragment (8 μM) at a flow rate of 1 μL/min (binding phase); and (c) 10 min of washing with running buffer at a flow rate of 10 μL/min (dissociation phase). All data were corrected for nonspecific binding of protein to the chip that was measured in control experiments without nickel.

RESULTS

Expression of Recombinant Protein Fragments of Filamin Isoforms. To determine the minimal region that is sufficient for filamin dimerization, a series of defined fragments derived from the carboxy-terminal portions of the three filamin isoforms characterized to date (for positions and nomenclature see Figure 1) were cloned into modified pET vectors. The purity of the recombinant filamin fragments is documented in Figure 2A, and their basic characteristics are summarized in Table 1.

All filamin fragments used in our experiments are composed essentially of Ig-like domains. Therefore, it was important to confirm that prokaryotically expressed fragments do not lose their capacity to fold into the characteristic β-barrel structure of Ig-like domains and that the addition of the different tags does not disturb correct folding. This was investigated by CD spectroscopy. A representative spectrum is shown in Figure 2B for the polypeptide fln c 23−24 (with His_6 and T7 tags). The molar extinction coefficient was determined to be $\epsilon = 17\,330\ M^{-1}\ cm^{-1}$. The CD spectrum in the far UV was reminiscent of that of other proteins of the intracellular branch of the immunoglobulin superfamily (*25*, *26*), which justified the assumption that our bacterially expressed proteins exhibited their native folding.

Conditions for Chemical Cross-Linking. Initially, optimal conditions for chemical cross-linking had to be established. For these experiments, the polypeptide fln c 23−24 was used at a concentration of 4 μmol/L. Figure 3A shows a concentration series with the bifunctional cross-linker ethylene glycol bis(succinimido succinate), EGS. Addition of the cross-linking reagent resulted in the appearance of a second band with lower gel mobility (~50 kDa instead of the ~30 kDa monomer). The intensity of this putative dimer band (marked d in Figure 3A) steadily increased proportionally to the EGS concentration in the reaction mixture. In the presence of 1.3 mM EGS, essentially all of the protein was recovered as dimer. Importantly, this 50 kDa band was recognized by an antibody directed against the immunotag of the recombinant protein (results not shown). Thus, we concluded that this band represented cross-linked dimers.

Likewise, we determined the optimal incubation time with this cross-linker (1.3 mM EGS) following dimerization. Figure 3B demonstrates that after an incubation time of only 1 s cross-linked dimers are already observed. After 5 min the majority of the dimers present in the protein solution were chemically cross-linked, and after 10 min the reaction was essentially complete. Thus, we used an EGS concentration of 1.3 mM for 20 min in all subsequent experiments to ensure a reliable and reproducible visualization of the

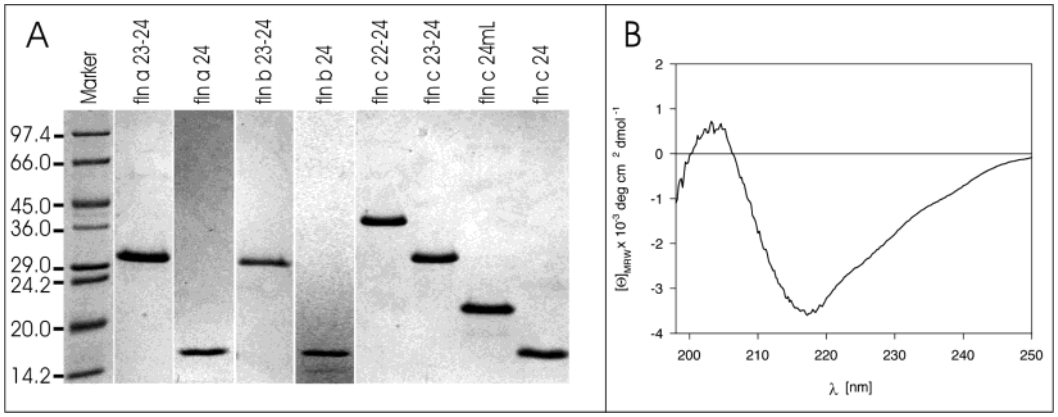

FIGURE 2: Analysis of purified filamin fragments used for dimerization studies. (A) Carboxy-terminal fragments of filamin a (fln a), filamin b (fln b), and filamin c (fln c), as marked above each lane, were expressed in *E. coli*, purified by Ni-NTA column chromatography, and analyzed on a 12% polyacrylamide gel. For the structure of the carboxy-terminal filamin fragments see Figure 1. (B) CD spectrum of fln c 23−24 in the far UV was performed with bacterially expressed filamin immunoglobulin domains. Note that the recombinant fragment shows the typical β-sheet secondary structure that has been predicted for filamin (*9*, *29*) suggesting proper folding. The ordinate gives the mean molar ellipticity (Θ_{MRW}).

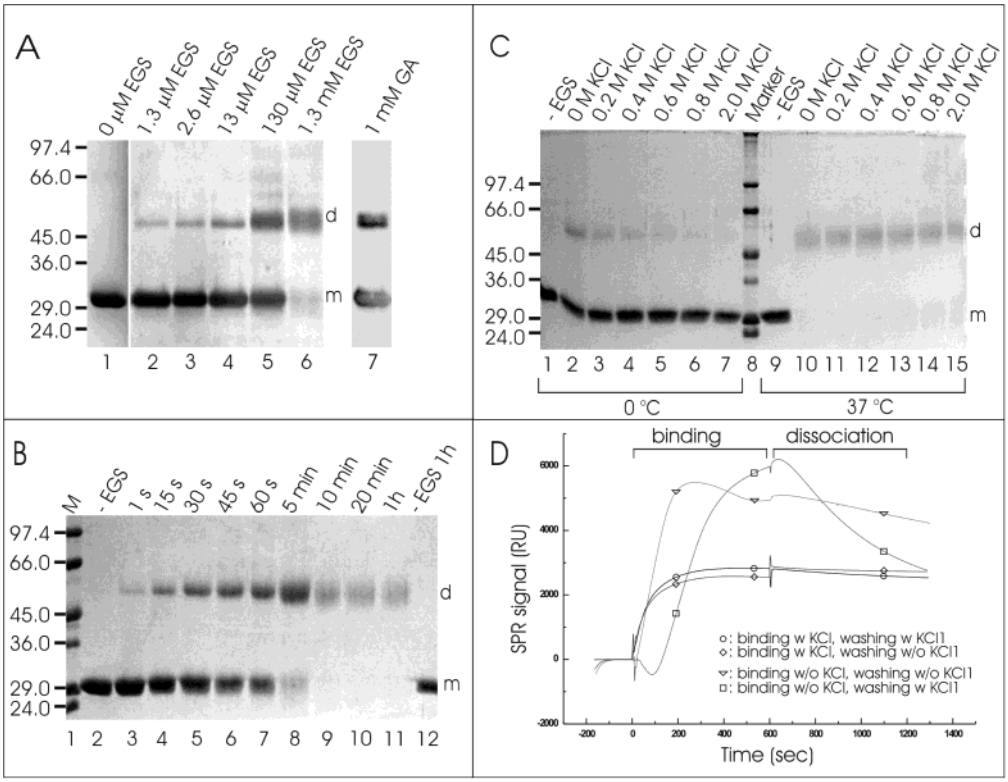

FIGURE 3: Establishing optimal conditions for chemical cross-linking experiments. (A) In a series of experiments the optimal concentration of the cross-linking agent ethylene glycol bis(succinimido succinate) (EGS), the time course, and the salt and temperature dependence of the reaction were established. Panel A shows the influence of the EGS concentration (as indicated above each lane) used in the reactions. The letter m emphasizes the position of the monomer in the gel, and d indicates the dimer. Molecular mass standards are indicated in kilodaltons at the left. Note that the efficiency of the dimerization is highly dependent on the EGS concentration. The use of glutaraldehyde as an alternative chemical cross-linker resulted in the detection of an identical dimer band (lane 7). (B) The minimum reaction time necessary for a complete cross-linking of protein fragments was determined. Without EGS, only monomers (lanes 2 and 12, m) are detected. Cross-linked dimers (d) are detectable after an incubation time in the presence of 1.3 mM EGS of only 1 s (lane 3). After 10 min, essentially all of the filamin fragment was cross-linked (lane 9). (C) Analysis of the effect of temperature and salt concentration on filamin dimerization. The concentration of KCl was adjusted to the values indicated on top of each lane, and each assay was incubated with 1.3 mM EGS. Samples were incubated either on ice or at 37 °C. The formation of cross-linked dimers (d) dramatically decreased at higher salt concentrations if incubated on ice. In contrast, an incubation at 37 °C yielded solely dimers independent of the salt concentration. (D) Surface plasmon resonance analysis of filamin dimerization with a Biacore 2000 instrument. SPR signals, corrected for unspecific binding of protein to the NTA chip without Ni ions, are given in response units (RU) and plotted against time. Recombinant histidine-tagged filamin c 24 was bound to the chip at a concentration of 8 μM in binding buffer with or without KCl, and the chip was washed with running buffer, with (w) or without (w/o) KCl as indicated. Note that in binding buffer without KCl the SPR signal is highly increased, reflecting dimer formation, and that the addition of KCl to the running buffer increases the dissociation velocity. In the latter case, the signal levels off at the monomer signal.

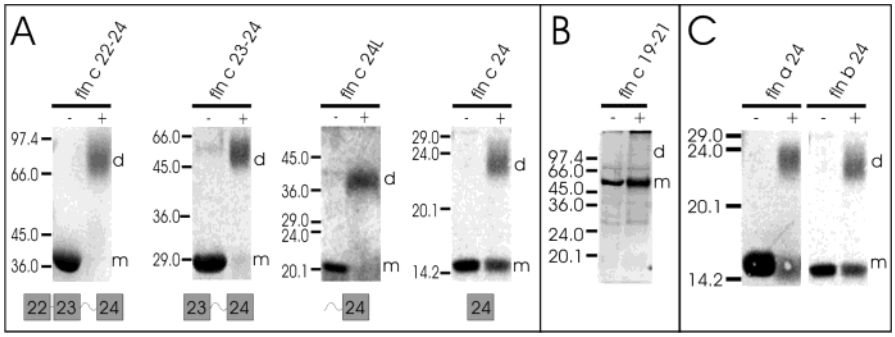

FIGURE 4: Analysis of chemical cross-linking of truncated filamin fragments by SDS−PAGE. Carboxy-terminal recombinant fragments derived from filamin a, b, or c as indicated above each lane were expressed in *E. coli* and purified. Presence or absence of the cross-linker EGS in the individual dimerization experiments is indicated above each lane by + or −, respectively. Cross-linked dimers (d) exhibited approximately twice the molecular mass of monomers (m). (A) Dimerization was evident with all filamin c polypeptides (depicted diagrammatically below each block of gels) containing at least the carboxy-terminal Ig-like domain. In contrast, a more amino-terminally located part of the protein fln c 19−21 showed no sign of dimerization (panel B). In panel C, the carboxy-terminally situated domains 24 of filamins a and b were used in a dimerization assay. Note that in both cases the amino-terminal Ig-like domain was sufficient for dimerization.

dimerization reaction. The specificity of this reaction was confirmed by substituting EGS with glutaraldehyde as an alternative cross-linker. These experiments consistently resulted in the same immunoreactive dimer bands (Figure 3A, lane 7).

Conditions That Favor the Formation of Filamin Monomers. To allow for the potential dimerization between distinct filamin isoforms, conditions were defined that favored filamin monomers rather than dimers. Two parameters that were modified to achieve this goal were salt concentration and temperature. Figure 3C shows results from cross-linking experiments with recombinant fln c 23−24 at two different temperatures and salt concentrations ranging from 0 to 2.0 M KCl. Filamin fragments were equilibrated for 1 h either on ice or at 37 °C. Subsequently, samples were incubated with 1.3 mM EGS for 20 min.

Incubation at 0 °C resulted in a strikingly lower yield of cross-linked dimers, when compared to the yield after an incubation at 37 °C. At this temperature a variation of the salt concentration had minimal effect on the dimerization efficiency: at all concentrations virtually all of the filamin fragment was recovered as dimers. At 0 °C a small but significant fraction of fln c 23−24 formed dimers at KCl concentrations of 0−0.4 M (Figure 3C). Upon a further increase of the salt concentration essentially no dimers were found. Thus, as an initial step in all subsequent dimerization experiments the recombinant polypeptides were preincubated on ice for 1 h in a buffer with a KCl concentration of 0.6 M.

Characterization of Dimerization and KCl Dependence on Dimerization by SPR. Binding experiments in a Biacore 2000 allowed the characterization of the dimerization state of the filamin domain by real-time monitoring of the quantity of recombinant polypeptide immobilized on the chip. Binding and elution of filamin c domain 24 was measured under four different conditions: the polypeptide was allowed to bind to saturation in binding buffer with or without 0.6 M KCl, and the chip was washed with running buffer with or without 0.6 M KCl. Since our cross-linking experiments showed that dimers were formed only at low KCl concentrations, we expected that dimerization as well as dissociation into monomers could be monitored due to the mass dependence of the SPR signal. A response unit (RU) of approximately 1000 equals a load of 1 ng/mm^2 on a sensor chip surface (*27*). Figure 3D shows the binding curves obtained at the different buffer conditions. When the recombinant filamin fragment was bound to the chip under conditions that favor dimerization (in buffer without KCl), signals of 5100−6200 RU (relative units) were obtained. Dilution of the same polypeptide in binding buffer containing 0.6 M KCl resulted in a decrease of the signal to approximately 2800 RU, i.e., half the value obtained in the experiments in which binding buffer without KCl was used. This lower value clearly indicated saturation of the chip with monomeric filamin fragment in high-salt buffer and saturation of the chip with dimerized filamin fragments in buffer without KCl. Thus, these results provide independent proof that single filamin domains are able to dimerize and that dimerization is not dependent on the presence of a cross-linking reagent.

We were not able to elute significant amounts of protein from the chips when filamin was bound under monomer favoring high-salt conditions, independent of the amount of KCl in the running buffer. In contrast, when dimerized filamin was bound to the chip, elution with high-salt running buffer resulted in a rapid decrease of the signal that eventually leveled off at the monomer signal, indicating complete monomerization. Interestingly, the dissociation rate of bound dimers in running buffer without KCl was significantly slower, confirming a high stability of the filamin dimers under these conditions. All these observations confirm our findings in the cross-linking experiments that monomers are favored in the presence of 0.6 M KCl.

The Carboxy-Terminal Ig Domain Is Sufficient for Dimerization. The shortest filamin fragment that enables dimer formation was established by a series of amino-terminal truncations (Figure 1). Polypeptides encompassing the carboxy-terminal three Ig-like domains 22−24, the two domains 23 and 24, the domain 24 plus the preceding hinge 2 region (polypeptide 24L), and solely domain 24 of filamin c were expressed in *E. coli*, purified, and analyzed for dimer formation as described above. Dimers were evident in all cases, indicating that domains 22 and 23 do not seem to play an important role in this process (Figure 4A). Though domain 24 alone could form dimers, it consistently failed to dimerize completely. Interestingly, the addition of the hinge 2 region to this domain (24L) led to a reconstitution of the ability to dimerize entirely. This observation indicates that the hinge

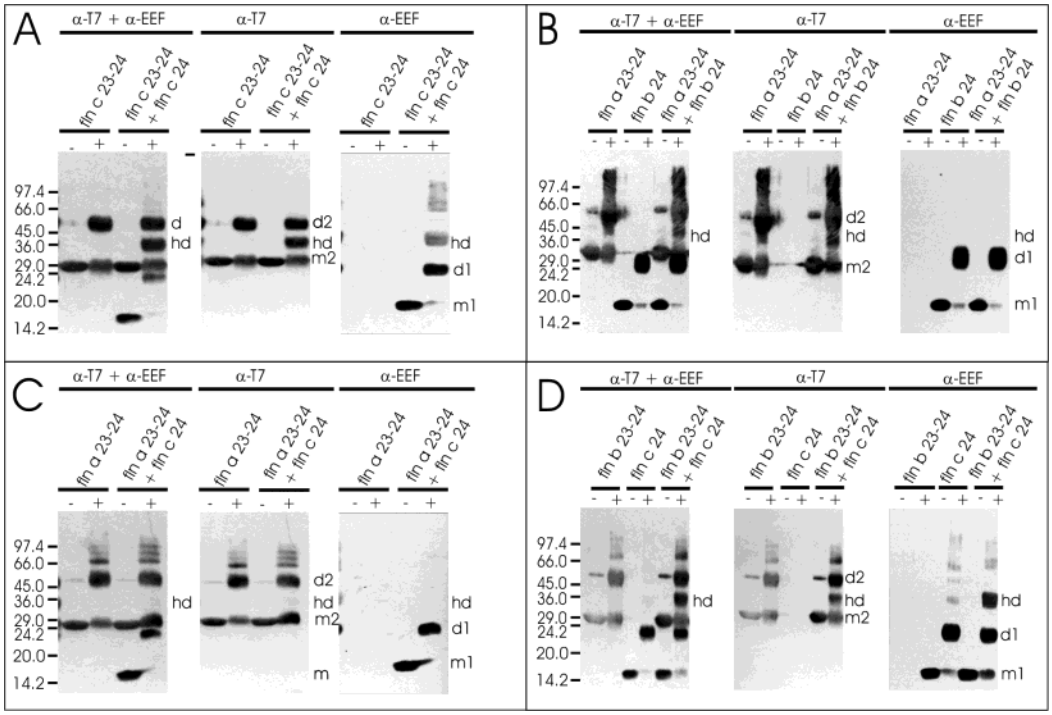

FIGURE 5: Heterodimerization of different filamin isoforms in vitro. Recombinant polypeptides derived from the carboxy termini of different filamin isoforms were mixed and incubated in the absence (−) or presence (+) of EGS. Proteins were separated by SDS−PAGE and blotted to PVDF. Membranes were incubated with antibodies specific for the T7 immunotag (α-T7), the EEF immunotag (α-EEF), or a combination of both antibodies (α-T7 + α-EEF) as indicated above the gel segments. Molecular mass marker positions are given in kilodaltons at the left of each figure. (A) Fln c 23−24 (T7 immunotag) cross-linked with fln c 24 (EEF immunotag). m1 and d1 mark the positions of monomers and dimers of the fragment fln c 23−24; m2 and d2 are monomers and dimers of fln c 24; hd emphasizes the heterodimer that is formed between both polypeptides. (B) Fln a 23−24 (T7-tagged) cross-linked with fln b 24 (EEF-tagged). m1 and d1 mark the positions of monomers and dimers of the polypeptide fln a 23−24; m2 and d2 are monomers and dimers of fln b 24; hd emphasizes the predicted position of the heterodimer between both polypeptides. (C) Fln a 23−24 (T7-tagged) and fln c 24 (EEF-tagged) were cross-linked and immunostained as indicated. m1 and d1 mark the positions of monomers and dimers of fln a 23−24; m2 and d2 are monomers and dimers of fln c 24. hd emphasizes the predicted position of the heterodimer. (D) Fln b 23−24 (T7-tagged) and fln c 24 (EEF-tagged) were cross-linked and immunostained as indicated. m1 and d1 mark the positions of monomers and dimers of fln b 23−24; m2 and d2 are monomers and dimers of fln c 24. hd emphasizes the heterodimer that is formed between both polypeptides. Note that heterodimers are only formed between filamins b and c but not between filamins a and c or filamins a and b.

2 region has a function in the control of filamin dimer formation.

As a further control, we expressed and purified a more amino-terminal filamin fragment that lacks domain 24 (fln c 19−21). This fragment showed no sign of dimerization (Figure 4B), confirming the correctness of the experimental setup and the importance of domain 24 for this process.

To compare the dimerization properties of all three human filamin isoforms, the carboxy-terminal domain of each isoform was expressed and purified. They were used for cross-linking studies as described above. Figure 4C shows that there are essentially no differences between the dimerization characteristics of the three filamin isoforms. Thus, we can conclude that the carboxy-terminal Ig domain is necessary and sufficient for filamin dimerization in all filamin isoforms. However, the preceding linker obviously exerts a regulatory or stabilizing role during this process.

Heterodimers Form between Filamins b and c but Not between Filamins a and b or a and c. In the experiments described above, we established conditions required for obtaining monomerized recombinant filamin fragments. This was a prerequisite to investigate the possibility whether protein fragments derived from different filamin isoforms could form heterodimers in solution. To discriminate between homodimers and heterodimers, we used in these chemical cross-linking experiments mixtures of the two-domain fragment 23−24 bearing an EEF tag or a T7 tag of one filamin isoform and the single-domain fragment 24 carrying a T7 tag or an EEF tag of another filamin isoform. The tags were chosen in such a way that potential heterodimers would have to be immunoreactive with both anti-EEF and anti-T7 antibodies. Furthermore, heterodimers should have an apparent molecular mass different from that of the homodimers that inevitably formed from the single-domain and the two-domain fragments. Thus, heterodimers were expected to be identifiable both by their immunoreactivity and by their distinct molecular mass.

Figure 5 shows the results of immunodetection and ECL reaction after cross-linking. To start with, the intrinsic possibility of one- and two-domain fragments of the same isoform to form dimers was confirmed. The presence of a heterodimer band (marked hd) with the expected molecular mass and the predicted immunoreactivities confirmed the dimerization of fln c 24 with fln c 23−24. Similar results were obtained with identical fragments from filamins a and b, respectively (not shown). Subsequently, the capability of forming heterodimers was analyzed with fragments derived from different filamin isoforms (Figure 5B−D). When filamin fragments fln b 23−24 (T7) and fln c 24 (EEF) were mixed under monomerizing conditions and subsequently incubated with EGS under conditions allowing dimerization, an additional protein band of approximately 36 kDa molec-

Table 2: Summary of the Results of the Cross-Linking Experiments[a]

	EEF-filamin a	EEF-filamin b	EEF-filamin c
T7-filamin a	+	−	−
T7-filamin b	−	+	+
T7-filamin c	−	+	+

[a] The possibility of forming homodimers or heterodimers is indicated by + and −, respectively. Note that filamin a only forms homodimers, whereas filamins b and c can form both homodimers and heterodimers.

ular mass (marked with hd in all panels of Figure 5D) appeared in immunoblots. This band was clearly distinct from those of the fln b 23−24 homodimer (d2, 50 kDa) and the fln c 24 homodimer (d1, 22 kDa). Its immunoreactivity with both anti-T7 (panel 2) and anti-EEF (panel 3) antibodies identified it unequivocally as a heterodimer. Identical results were obtained with fln b 24 and fln c 23−24 fragments (not shown). In contrast, filamin a seemed to be incapable of forming dimers with any of the other isoforms. In all experiments that included this isoform, only homodimers of the respective polypeptides were cross-linked (Figure 5B,C). The results of the cross-linking data are summarized in Table 2.

DISCUSSION

Filamins are a family of closely related high molecular mass actin-binding proteins that seem to be ubiquitously distributed, at least among higher vertebrate cells. Filamins have been described in conjunction with the actin cytoskeleton at locations as diverse as stress fibers, microspikes, cleavage furrows, meshworks, or the sarcomeric Z-disk. In vitro, filamins are capable of organizing actin filaments either into meshworks or bundles, depending on the stoichiometry of filamin to actin (see ref 28 and references therein). The actin cross-linking activity is explained by the structural layout of the filamin molecule in which an amino-terminal actin-binding domain is followed by 24 Ig-like modules (see also Figure 1). The carboxy-terminal part of the molecule is involved in dimerization. The resulting Y-shaped dimerized molecules with actin-binding sites at both ends (*9*) are perfectly suited to link actin filaments into bundles or meshworks.

Mapping of the region involved in dimer formation has been achieved only to a certain degree, and many of the approaches were of a relatively indirect nature. For example, limited proteolysis of chicken smooth muscle filamin yielded a 240 kDa amino-terminal fragment that was still capable of binding to F-actin but that had lost its actin-gelling activity. Therefore, it was concluded that the ability to dimerize should reside in the carboxy-terminal portion that was cleaved off (*16*). Weihing (*17*) showed that upon proteolytic cleavage of filamin purified from HeLa cells the 104 kDa carboxy-terminal fragment was responsible for dimerization. Cleavage of human smooth muscle filamin by a calcium-activated protease into an amino-terminal 220 kDa actin-binding fragment and a carboxy-terminal 35 kDa fragment, followed by gel-filtration analysis, indicated that the latter eluted as a dimer (*29*). The nature of the dimerization or the structure of the domains involved in dimerization remained unclear. cDNA cloning finally elucidated the overall molecular structure of human nonmuscle filamin and showed that it is largely built of globular Ig-like domains (*9*; for a schematic representation see Figure 1), whose three-dimensional structure was recently revealed at the atomic level for the related *Dictyostelium* protein ABP120 (*30*, *31*). At two positions the filamin molecule is interrupted by nonmodular insertions, called hinges, which were found to be particularly sensitive to proteolysis. When filamin was cleaved at the second hinge, i.e., just prior to Ig-like domain 24, the resulting large amino-terminal fragment remained monomeric, implying that domain 24 was at least *required* for dimerization (*9*). In the same report the authors demonstrated by chemical cross-linking that a recombinant fragment comprising half of domain 21 and the carboxy-terminal remainder of the filamin polypeptide could be cross-linked, whereas a second fragment that lacked the extreme carboxy-terminal 65 amino acids could not (*9*). These data did, however, not reveal whether the Ig-like domain 24 *alone* was *sufficient* for dimerization or if a bigger portion was in fact required. Our cross-linking experiments presented in this report unequivocally show that the carboxy-terminal domains of all three filamins are already capable of forming cross-linkable dimers. Interestingly, this capability is significantly enhanced if the preceding hinge 2 region is included in the fragments used (Figure 5), implying a yet unknown regulatory mechanism for the fine regulation of filamin dimerization. In this respect it is interesting to note that phosphorylation of chicken gizzard filamin by Ca^{2+}/calmodulin-dependent protein kinase, whose phosphorylation site was predicted to be in the hinge 2 region (*9*), resulted in decreased actin binding as shown by sedimentation assays (*32*). Furthermore, phosphorylation of muscle and nonmuscle filamins dramatically reduced binding of both filamin isoforms to myofibrils (*33*), and filamin phosphorylation by Ca^{2+}/calmodulin-dependent protein kinase seems to be involved in translocation processes in endothelial cells (*34*, *35*).

In the related molecule ABP120 (*Dictyostelium* gelation factor), the crystal structure of the two carboxy-terminal domains revealed that ABP120 molecules overlap only with domain 6, in an antiparallel way (*31*). This indicated that in the *Dictyostelium* protein this single domain is sufficient for dimerization. These results, however, do not give the desired information about a possible function for the hinge region between the two carboxy-terminal domains. Furthermore, although this protein is related to the vertebrate filamins, there are marked differences between the dimerizing domains of both kinds of proteins, not only at the level of the primary sequence. In addition, the parallel arrangement of the filamin chains in the dimers implied by electron micrographs (*9*, *15*, *16*) point to an alternative mechanism of dimerization. Surprisingly, a comparison of the structures predicted for the dimerizing domains of all three human filamins (see Figure 6) with the structures of ABP120 domains 4, 5, and 6 that were established by X-ray crystallography (*30*, *31*) indicated that the homology with the nondimerizing domain 4 is more pronounced than the similarity to domains 5 and 6 (Figure 6). These predictions imply a different dimerization mechanism, as was already suggested in the paper that described the structure of dimerized ABP120, and strengthens the relevance of our study.

A further level of complexity to the filamin family was added by the finding that in the human genome there are at least three distinct filamin genes, each giving rise to several

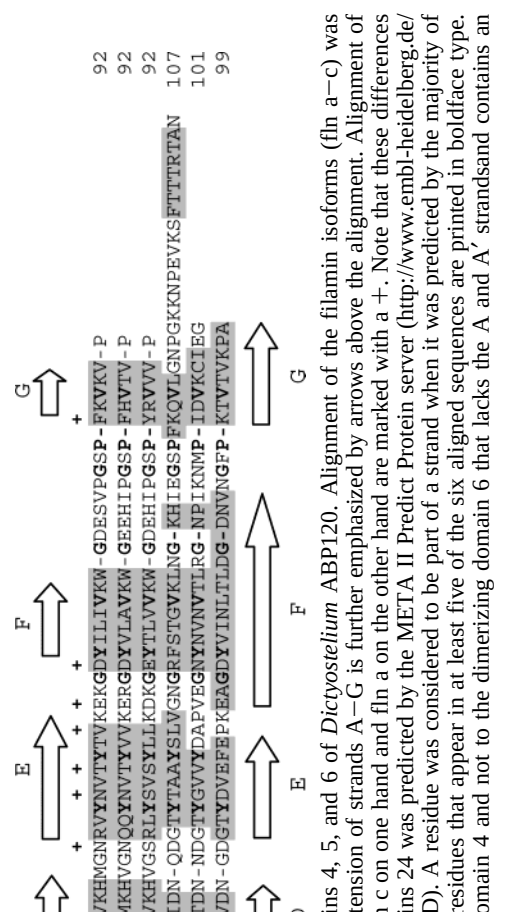

FIGURE 6: Sequence alignment of Ig domain 24 of the human filamins a, b, and c and the Ig domains 4, 5, and 6 of *Dictyostelium* ABP120. Alignment of the filamin isoforms (fln a−c) was performed with BioEdit 5.0.9 (*45*). Amino acid residues comprising a *β*-strand are shaded and the extension of strands A−G is further emphasized by arrows above the alignment. Alignment of the ABP120 domains 4−6 (dict 4−6) was done according to ref 31. Differences between fln b and fln c on one hand and fln a on the other hand are marked with a +. Note that these differences are clustered in the predicted E strand and its neighboring loops. The structure of the filamin Ig domains 24 was predicted by the META II Predict Protein server (http://www.embl-heidelberg.de/predictprotein) and servers linked to this server (APSSP2, UCSC SAM-T99, JPRED2, PROF, PSIRED). A residue was considered to be part of a strand when it was predicted by the majority of the programs. Alignment of the filamins with ABP120 was also performed with BioEdit. Conserved residues that appear in at least five of the six aligned sequences are printed in boldface type. Note that the predicted secondary structure of the filamins is most homologous to that of ABP120 domain 4 and not to the dimerizing domain 6 that lacks the A and A′ strandsand contains an F′ strand and an extra H strand (see also ref 29a).

splice variants (*6*, *11*, *36*, *37*). Importantly, however, until now no differential splicing has been observed in the carboxy-terminal portions, which were shown to be involved in dimerization in this report. Thus, it is most likely that our results reflect a fundamental mechanism. But what if different isoforms are expressed simultaneously in a cell? Such a phenomenon was shown to occur in HeLa cells by peptide mapping (*38*) and in retinal pericytes by Western blotting (*39*). Filamin isoform expression was also studied by in situ hybridization on mouse embryo sections, which showed coexpression of filamin isoforms in some cell types at the mRNA level (*40*). Thus the question arises whether at the molecular level a sorting mechanism exists that would direct isoform-specific homodimerization as opposed to promiscuous heterodimerization. Both possibilities have immediate functional implications, because distinct filamins have variously been shown to be involved in linking submembranous actin cortical filaments to specific cell surface proteins (for recent reviews see refs 2 and 3). Heterodimerization might link the ligand of one filamin isoform to the ligand of the second isoform, which would increase the complexity of the filamin family and its possible functions.

Coexpression of different filamin isoforms was also described for developing avian (*41*, *42*) and human (*18*) striated muscle. In differentiating cultured muscle cells it has been shown that filamin a and filamin c are coexpressed in early myotubes. For a limited period of time, both isoforms can be detected in Z-bodies, periodic structures in premature myofibrils that already contain several Z-disk proteins (*43*). During further differentiation, Z-bodies of neighboring myofibrils fuse to form mature Z-disks (*44*). During this process, filamin a gradually disappears from the developing myofibrils and is replaced by filamin c (*18*). A mechanism that could theoretically be involved in this isoform switching is the transient assembly of heterodimers of filamin a and filamin c molecules. Our dimerization experiments, however, show that these two filamin isoforms are not capable of forming heterodimers, at least in vitro, indicating that isoform switching cannot be accompanied by a transitory heterodimerization of both filamin isoforms. Furthermore, the observation that filamin a is capable of binding to myofibrillar Z-disks, although it is not found in striated muscle cells in vivo (*33*), cannot be explained by a heterodimerization with filamin c molecules.

Thus, our results pose certain limits on the theoretically possible filamin-dimer variability. The almost ubiquitously distributed filamin a can—at least under the conditions of our cross-linking experiments—only form homodimers. In contrast, filamins b and c are also capable of forming heterodimers (see Figure 5). A comparison of the primary and predicted secondary structure of the filamins shows that all three isoforms have highly similar structures. Interestingly, in the predicted E strand, that in domains with an Ig-like fold forms a sheet together with the B- and D-strands, filamins b and c show a significantly higher mutual homology when compared to filamin a (Figure 6). Thus, six out of 15 residues that comprise strand E and its flanking loops are only shared by filamins b and c, while in the remaining 77 amino acids merely three residues are specific for these filamin isoforms (compare residues indicated by + in Figure 6). We speculate that this phenomenon is causative for the inability of filamin a to heterodimerize with both other

filamin isoforms and that this particular sheet must play an important role in filamin dimerization. Direct proof for the precise mechanism of filamin dimer formation will have to await crystallization studies. The same holds true for the observed role of the hinge 2 region in the regulation and/or stabilization of filamin dimerization. The parallel arrangement of neighboring filamin molecules places the hinge region of one molecule in immediate contact with the second molecule in the dimer, which would permit a function in dimerization. It is intriguing to assume that the observed regulation of filamin activity by phosphorylation of the hinge 2 region as described above (*9*, *32*) is originated by an alteration of the dimerization capacity of the molecule. In contrast, the antiparallel overlap of two ABP120 molecules makes this possibility highly improbable.

Unfortunately, the antibodies that recognize filamins b and c described to date are either not isoform-specific or not very adequate for microscopy. Thus, to establish whether in a living cell filamins b and c occur in distinct or overlapping compartments and to clarify whether heterodimerization between filamins b and c has a physiological function, novel isoform-specific antibodies need to be developed for application in high-resolution microscopy.

ACKNOWLEDGMENT

We thank Drs. Shapiro and Takafuta (Cardeza Foundation for Hematologic Research, Jefferson Medical College, Philadelphia, PA) for donation of the filamin b cDNA, Dr. J. Wehland, Braunschweig, Germany, for donation of the YL1/2 antibody, and Dr. U. Baxa (Department of Physical Biochemistry, University of Potsdam) for help with the CD spectra. Dr. Thomas P. Stossel is thanked for helpful discussions. The involvement of Britt Lemke (Max-Delbrück-Centre, Berlin) in the initial stages of the project is gratefully acknowledged.

REFERENCES

1. Gimona, M., Djinovic-Carugo, K., Kranewitter, W. J., and Winder, S. J. (2002) Functional plasticity of CH domains, *FEBS Lett. 513*, 98−106.
2. Stossel, T. P., Condeelis, J., Cooley, L., Hartwig, J. H., Noegel, A., Schleicher, M., and Shapiro, S. S. (2001) Filamins as integrators of cell mechanics and signaling, *Nat. Rev. Mol. Cell. Biol. 2*, 138−145.
3. Van der Flier, A., and Sonnenberg, A. (2001) Structural and functional aspects of filamins, *Biochim. Biophys. Acta 1538*, 99−117.
4. Fox, J. W., Lamperti, E. D., Eksioglu, Y. Z., Hong, S. E., Feng, Y., Graham, D. A., Scheffer, I. E., Dobyns, W. B., Hirsch, B. A., Radtke, R. A., Berkovic, S. F., Huttenlocher, P. R., and Walsh, C. (1998) Mutations in filamin 1 prevent migration of cerebral cortical neurons in human periventricular heterotopia, *Neuron 21*, 1315−1325.
5. Speer, M. C., Vance, J. M., Grubber, J. M., Graham, F. L., Stajich, J. M., Viles, K. D., Rogala, A., McMichael, R., Chutkow, J., Goldsmith, C., Tim, R. W., and Pericak-Vance, A. (1999) Identification of a new autosomal dominant limb-girdle muscular dystrophy locus on chromosome 7, *Am. J. Hum. Genet. 64*, 556−562.
6. Chakharova, C., Wehnert, M. S., Uhl, K., Sakthivel, S., Vosberg, H.-P., van der Ven P. F. M., and Fürst, D. O. (2000) Genomic structure and fine mapping of the two filamin gene paralogues FLNB and FLNC and comparative analysis of the filamin gene family, *Hum. Genet. 107*, 597−611.
7. Hartwig, J. H. and Stossel, T. P. (1975) Isolation and properties of actin, myosin, and a new actin binding protein in rabbit alveolar macrophages, *J. Biol. Chem. 250*, 5696−5705.
8. Wang, K., Ash, J. F., and Singer, S. J. (1975) Filamin, a new high-molecular-weight protein found in smooth muscle and nonmuscle cells, *Proc. Natl. Acad. Sci. U.S.A. 72*, 4483−4486.
9. Gorlin, J. B., Yamin, R., Egan, S., Stewart, M., Stossel, T. P., Kwiatkowski, D. J., and Hartwig, J. H. (1990) Human endothelial actin-binding protein (ABP-280, nonmuscle filamin): a molecular leaf spring, *J. Cell Biol. 111*, 1089−1105.
10. Takafuta T., Wu, G., Murphy, G. F., and Shapiro, S. S. (1998) Human beta-filamin is a new protein that interacts with the cytoplasmic tail of glycoprotein Ib alpha, *J. Biol. Chem. 273*, 17531−17538.
11. Xu, W. F., Xie, Z., Chung, D. W., and Davie, E. W. (1998) A novel human actin-binding protein homologue that binds to platelet glycoprotein Ib alpha, *Blood 92*, 1268−1276.
12. Zhang, W., Han, S. W., McKeel, D. W., Goate, A., and Wu, J. Y. (1998) Interaction of presenilins with the filamin family of actin-binding proteins, *J. Neurosci. 18*, 914−922.
13. Maestrini, E., Patrosso, C., Mancini, M., Rivella,, Rocchi, M., Repetto, M., Villa, A., Frattini, A., Zoppé, M., Vezzoni, P., and Toniolo, D. (1993) Mapping of two genes encoding isoforms of the actin binding protein ABP-280, a dystrophin like protein, to Xq28 and to chromosome 7, *Hum. Mol. Genet. 2*, 761−766.
14. Xie, Z, Xu, W., Davie, E. W., and Chung, D. W. (1998) Molecular cloning of human ABPL, an actin-binding protein homologue, *Biochem. Biophys. Res. Commun. 251*, 914−919.
15. Tyler, J. M., Anderson, J. M., and Branton, D. (1980) Structural comparison of several actin-binding macromolecules, *J. Cell Biol. 85*, 489−95.
16. Davies, P. J. A., Wallach, D., Willingham, M., Pastan, I., and Lewis, M. S. (1980) Self-association of chicken gizzard filamin and heavy merofilamin, *Biochemistry 19*, 1366−1372.
17. Weihing, R. R. (1988). Actin-binding and dimerization domains of HeLa cell filamin, *Biochemistry 27*, 1865−1869.
18. Van der Ven, P. F. M., Obermann, W. M. J., Lemke, B., Gautel, M., Weber, K., and Fürst, D. O. (2000) The characterization of muscle filamin isoforms suggests a possible role of ABP-L/γ-filamin in sarcomeric Z-disc formation, *Cell Motil. Cytoskeleton 45*, 149−162.
19. Obermann, W., Gautel, M., Steiner, F., van der Ven, P. F. M., Weber, K., and Fürst, D. O. (1996) Molecular structure of the sarcomeric M band: localization of defined domains of myomesin, M-protein and the 250 kDa carboxyterminal region of titin, *J. Cell Biol. 134*, 1441−1453.
20. Obermann, W. M. J., van der Ven, P. F. M., Steiner, F., Weber, K., and Fürst, D. O. (1998) Mapping of a myosin-binding domain and a regulatory phosphorylation site in M-protein, a structural protein of the sarcomeric M band, *Mol. Biol. Cell 9*, 829−840.
21. Wehland, J., Willingham, M. C., and Sandoval, I. V. (1983) A rat monoclonal antibody reacting specifically with the tyrosylated form of alpha-tubulin. I. Biochemical characterization, effects on microtubule polymerization in vitro, and microtubule polymerization and organization in vivo, *J. Cell Biol. 97*, 1467−1475.
22. Obermann, W., Gautel, M., Weber, K., and Fürst, D. O. (1997) Molecular structure of the sarcomeric M band: mapping of titin and myosin binding domains in myomesin and the identification of a potential regulatory phosphorylation site in myomesin, *EMBO J. 16*, 211−220.
23. Pace, C. N., Vajdos, F., Fee, L., Grimsley, G., and Gray, T. (1995) How to measure and predict the molar absorption coefficient of a protein, *Protein Sci. 4*, 2411−2423.
24. Laemmli, U.K. (1970) Cleavage of structural proteins during the assembly of the head of bacteriophage T4, *Nature 227*, 680−685.
25. Nave, R., Fürst, D. O., Vinkemeier, U., and Weber, K. (1991) Purification and physical properties of nematode mini-titin and their relation to twitchin, *J. Cell Sci. 98*, 491−496.
26. Fürst, D. O., Vinkemeier, U., and Weber, K. (1992) Mammalian skeletal muscle C-protein: purification from bovine muscle, binding to titin and the characterization of a full-length human cDNA, *J. Cell Sci. 102*, 769−778.
27. Stenberg, E., Persson, B., Roos, H., Urbaniczky, C. (1991) Quantitative determination of surface concentration of protein with surface plasmon resonance using radiolabeled proteins, *J. Colloid Interface Sci. 143*, 513−526.
28. Hock, R. S. (1999) Filamin, in *Guidebook to the Cytoskeletal and Motor Proteins* (Kreis T., and Vale, R., Eds.) pp 94−97, Oxford University Press, Oxford, England.

29. Hock, R. S., Davis, G., and Speicher, D. W. (1990) Purification of human smooth muscle filamin and characterization of structural domains and functional sites, *Biochemistry 29*, 9441−9451.
30. Fucini, P., Renner, C., Herberhold, C., Noegel, A. A., and Holak, T. A. (1997) The repeating segments of the F-actin cross-linking gelation factor (ABP120) have an immunoglobulin-like fold, *Nat. Struct. Biol. 4*, 223−230.
31. McCoy, A. J., Fucini, P., Noegel, A. A., and Stewart, M. (1999) Structural basis for dimerization of the dictyostelium gelation factor (ABP120) rod, *Nat. Struct. Biol. 6*, 836−841.
32. Ohta, Y., and Hartwig, J. H. (1995) Actin filament cross-linking by chicken gizzard filamin is regulated by phosphorylation in vitro, *Biochemistry 34*, 6745−6754.
33. Chiang, W., and Greaser, M. L. (2000) Binding of filamins to myofibrils, *J. Muscle Res. Cell Motil. 21*, 321−333.
34. Hastie, L. E., Patton, W. F., Hechtman, H. B., and Shepro, D. (1997) H_2O_2-induced filamin redistribution in endothelial cells is modulated by the cyclic AMP-dependent protein kinase pathway, *J. Cell. Physiol. 172*, 373−381.
35. Wang, Q., Patton, W. F., Chiang, E. T., Hechtman, H. B., and Shepro, D. (1996) Filamin translocation is an early endothelial cell inflammatory response to bradykinin: regulation by calcium, protein kinases, and protein phosphatases, *J. Cell. Biochem. 62*, 383−396.
36. Gariboldi, M., Maestrini, E., Canziani, F., Manenti, G., De Gregorio, L., Rivella, S., Chatterjee, A., Herman, G. E., Archidiacono, N., Antonacci, R., Pierotti, M. A., Dragani, T. A., and Toniolo, D. (1994) Comparative mapping of the actin-binding protein 280 genes in human and mouse, *Genomics 21*, 428−430.
37. Van der Flier, A., Kuikman, I., Kramer, D., Geerts, D., Kreft, M., Takafuta, T., Shapiro, S. S., and Sonnenberg, A. (2002) Different splice variants of filamin-B affect myogenesis, subcellular distribution, and determine binding to integrin β subunits, *J. Cell Biol. 156*, 361−376.
38. Mangeat, P. H., and Burridge, K. (1983) Binding of HeLa spectrin to a specific HeLa membrane fraction, *Cell Motil. 3*, 657−666.
39. Shojaee, N., Patton, W. F., Chung-Welch, N., Su, Q., Hechtman, H. B., and Shepro, D. (1998) Expression and subcellular distribution of filamin isotypes in endothelial cells and pericytes, *Electrophoresis 19*, 323−332.
40. Chiang, W., Greaser, M. L., and Lyons, G. E. (2000) Filamin isogene expression during mouse myogenesis, *Dev. Dyn. 217*, 99−108.
41. Gomer R. H., and Lazarides, E. (1983) Highly homologous filamin polypeptides have different distributions in avian slow and fast muscle fibers, *J. Cell Biol. 97*, 818−823.
42. Price, M. G., Caprette, D. R., and Gomer, R. H. (1994) Different temporal patterns of expression result in the same type, amount, and distribution of filamin (ABP) in cardiac and skeletal myofibrils, *Cell Motil. Cytoskeleton 27*, 248−61.
43. Rhee, D., Sanger, J. M., and Sanger, J. W. (1994) The premyofibril: evidence for its role in myofibrillogenesis, *Cell Motil. Cytoskeleton 28*, 1−24.
44. Dabiri, G. A., Turnacioglu, K. K., Sanger, J. M., and Sanger, J. W. (1997) Myofibrillogenesis visualized in living embryonic cardiomyocytes, *Proc. Natl. Acad. Sci. U.S.A. 94*, 9493−9498.
45. Hall, T. A. (1999) BioEdit: a user-friendly biological sequence alignment editor and analysis program for Windows 95/98/NT, *Nucleic Acids Symp. Ser. 41*, 95−98.

BI026501+